

## Electronic states of charge-ordering $\text{Nd}_{0.5}\text{Sr}_{0.5}\text{MnO}_3$ probed by photoemission

A. Sekiyama, S. Suga, M. Fujikawa, S. Imada, T. Iwasaki, K. Matsuda,  
and T. Matsushita\*

*Department of Material Physics, Faculty of Engineering Science, Osaka University, Toyonaka, Osaka 560-8531, Japan*

K. V. Kaznachev

*Department of Physics and Astronomy, State University of New York, Stony Brook, New York 11794*

A. Fujimori

*Department of Physics, University of Tokyo, Bunkyo-ku, Tokyo 113-0033, Japan*

H. Kuwahara<sup>†</sup>

*Joint Research Center for Atom Technology (JRCAT), Tsukuba 305-0046, Japan*

Y. Tokura

*Joint Research Center for Atom Technology (JRCAT), Tsukuba 305-0046, Japan  
and Department of Applied Physics, University of Tokyo, Bunkyo-ku, Tokyo 113-8656, Japan*

(Received 10 November 1998; revised manuscript received 19 January 1999)

Electronic structures of the charge-ordering manganite  $\text{Nd}_{1-x}\text{Sr}_x\text{MnO}_3$  ( $x \sim 0.5$ ) have been studied by resonant and high-resolution photoemission. The Mn  $2p$  (Nd  $3d$ ) resonant photoemission confirmed the Mn  $3d$  (Nd  $4f$ ) states hybridized with the O  $2p$  states. The high-resolution Mn  $3p$  resonance spectra show a clear transition from the metal to the charge-ordered insulator for  $x=0.5$  upon cooling while a Fermi cutoff is seen for  $x=0.47$  at all temperatures, suggesting that the transition is induced by a subtle competition between the charge-ordering instability and the double-exchange interaction. Temperature and filling dependence of the spectra implies that the electronic states change not gradually but suddenly at the phase boundary. [S0163-1829(99)09623-X]

### I. INTRODUCTION

The manganese-based perovskite oxides have attracted great interest due to the recent discovery of colossal magnetoresistance.<sup>1,2</sup> As well known,  $\text{LaMnO}_3$  is an A-type antiferromagnetic insulator (AFI),<sup>2,3</sup> in which two kinds of distortion, namely, the  $\text{GdFeO}_3$ -type and the Jahn-Teller (JT) type, are involved.  $\text{La}_{1-x}\text{Sr}_x\text{MnO}_3$ <sup>2</sup> undergo a transition from the AFI to a ferromagnetic metal (FM) by carrier-doping and a transition from a paramagnetic insulator (PI) to the FM upon cooling for  $x > 0.15$ . These magnetic and transport properties have been explained by the double-exchange (DE) mechanism.<sup>4</sup> Recently, it has been pointed out that the dynamic JT effect is important in addition to the DE interaction.<sup>5</sup> On the other hand, it has been found that some perovskite manganites with commensurate values of  $x$ , such as  $\text{Nd}_{0.5}\text{Sr}_{0.5}\text{MnO}_3$ ,<sup>6,7</sup> undergo a transition from the FM to a charge-ordered insulator (COI) upon cooling. The FM-COI transition is accompanied by a spin- and orbital-ordering, and it is also known that a charge-exchange (CE)-type antiferromagnetic structure<sup>3</sup> is realized in the COI phase.<sup>8</sup> Since  $\text{La}_{0.5}\text{Sr}_{0.5}\text{MnO}_3$  is ferromagnetically metallic below the Curie temperature ( $T_c$ ),<sup>2</sup> the COI phase in  $\text{Nd}_{0.5}\text{Sr}_{0.5}\text{MnO}_3$  is considered to be stabilized by the larger  $\text{GdFeO}_3$ -type distortion (smaller Mn-O-Mn bonding angle) than in  $\text{La}_{0.5}\text{Sr}_{0.5}\text{MnO}_3$ , arising from the difference between the ionic radii of the atoms at the A-sites.<sup>7</sup> Although many photoemission studies on the perovskite manganites have been reported,<sup>9-14</sup> a spec-

tral change from the FM to the CE-type COI phase have not been observed so far. On the other hand, the magnetic circular dichroism of core absorption spectra of manganites has shown the rare-earth  $4f$  and  $5d$  states are hybridized with the conduction-band states.<sup>15</sup> Therefore, the photoemission study of the rare-earth  $4f$  contributions in the whole valence-band regions is needed to discuss the electronic states in the manganites. However, such an experimental study is still lacking for  $R_{1-x}\text{Sr}_x\text{MnO}_3$  ( $R = \text{Pr}, \text{Nd}, \text{and Sm}$ ).

In this paper, we report on resonant and high-resolution photoemission studies on  $\text{Nd}_{1-x}\text{Sr}_x\text{MnO}_3$  with  $x=0.47$  and  $0.5$  in order to clarify the electronic structures in the whole valence-band region and near the Fermi level ( $E_F$ ).  $\text{Nd}_{0.5}\text{Sr}_{0.5}\text{MnO}_3$  ( $x=0.5$ ) undergoes a PI-FM transition at  $T_c \sim 255$  K and a FM-COI transition at  $T_{COI} \sim 158$  K upon cooling.<sup>6</sup>  $\text{Nd}_{0.53}\text{Sr}_{0.47}\text{MnO}_3$  ( $x=0.47$ ) is in the FM phase below  $T_c \sim 275$  K and does not exhibit any COI transition.<sup>16</sup> Resonant photoemission spectra have clearly revealed the Nd  $4f$  and Mn  $3d$  electronic states. High-resolution photoemission spectra have shown clear difference of the electronic states due to a small deviation of composition. Namely, the spectra for  $x=0.5$  show spectral change across the FM-COI transition while a Fermi cutoff is seen for  $x=0.47$  at all temperatures. Furthermore, we discuss temperature and filling dependence of the spectra and the spectral line shapes, comparing our results on  $\text{Nd}_{1-x}\text{Sr}_x\text{MnO}_3$  with the previously reported spectra of the other manganites.

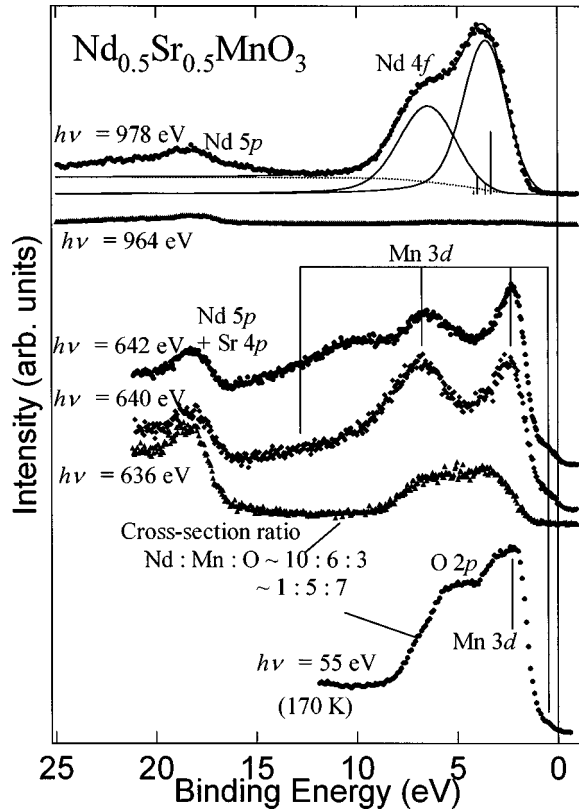


FIG. 1. Comparison of the valence-band spectra of  $\text{Nd}_{0.5}\text{Sr}_{0.5}\text{MnO}_3$  taken at various photon energies including the Mn  $2p$  and Nd  $3d$  resonant spectra.

## II. EXPERIMENT

Single-crystal samples were grown by the floating-zone method.<sup>6</sup> Mn  $2p$ - $3d$  and Nd  $3d$ - $4f$  resonant photoemission was performed at 300 K at beam line BL-2B of the Photon Factory (PF),<sup>17</sup> High-Energy Accelerator Research Organization. The energy resolution was  $<0.8$  and  $\sim 1.0$  eV, respectively. In order to obtain clean surfaces, the sample surfaces were repeatedly scraped *in situ* with a diamond file. High-resolution photoemission measurements ( $h\nu=55$  eV) were done at beam line BL-3B of PF (Ref. 18) at various temperatures with the total energy resolution of  $\sim 45$  meV. The samples were fractured *in situ* and the high-resolution spectra were measured within 1 h to avoid surface degradation. The fractured surfaces were irregular and the obtained spectra showed no angular dependence.  $h\nu=55$  eV corresponds to an energy that is a little higher than the Mn  $3p$  absorption threshold. The base pressure was  $\sim 3 \times 10^{-10}$  Torr. All measurements were repeated to ensure reproducibility of the spectra.

## III. RESULTS AND DISCUSSION

### A. Resonant photoemission spectra in the entire valence-band region

Photoemission spectra of  $\text{Nd}_{0.5}\text{Sr}_{0.5}\text{MnO}_3$  in the entire valence-band region are shown in Fig. 1. The spectra taken at  $h\nu=978$  (642) and 964 eV (636 eV) correspond to the Nd  $3d$ - $4f$  (Mn  $2p$ - $3d$ ) resonance maximum and minimum, respectively. The spectra are normalized to the photon flux

estimated from the mirror current of the monochromator for each set of the resonant photoemission spectra. A two-peak structure is observed at  $\sim 3.5$  and  $\sim 7$  eV in the Nd  $3d$ - $4f$  resonance-maximum spectrum, which is characteristic of a localized  $4f^3$  ground state and similar to that in the previously reported Nd  $4d$ - $4f$  resonant spectrum of  $\text{Nd}_{1.8}\text{Ce}_{0.2}\text{CuO}_4$ .<sup>19</sup> From a cluster model analysis,<sup>20</sup> the unhybridized  $f$ -hole ( $-\varepsilon_f$ ) and ligand-hole ( $-\varepsilon_L$ ) energies, and the effective transfer integral  $\sqrt{12}V$  have been estimated as  $4.7 \pm 0.2$ ,  $5.1 \pm 0.4$ , and  $1.35 \pm 0.05$  eV, respectively. These results indicate that the O  $2p$  states that can be hybridized with the Nd  $4f$  orbitals are located near the bare Nd  $4f$  levels and hence the Nd  $4f$ -O  $2p$  hybridization effect in the final states is strong. In the Mn  $2p$ - $3d$  resonant spectra ( $h\nu=640$  and 642 eV), Mn  $3d$ -derived spectral features appear at  $\sim 0.6$ , 2.3, and 6.7 eV. The spectral line shape is qualitatively similar to those reported by Park *et al.*<sup>12</sup> The 0.6 eV shoulder and 2.3 eV peak, which are also clarified in the spectrum taken at  $h\nu=55$  eV, are ascribed to the  $e_g$  and  $t_{2g}$  states, respectively. These results are fairly consistent with the band-structure calculation of  $\text{LaMnO}_3$  (Ref. 21) done using the local-spin density approximation (LSDA) if we assume that the structure of the Mn  $3d$  band does not change much by the hole doping. The 6.7 eV peak corresponds to the  $t_{2g}$  states strongly hybridized with the O  $2p$  states, which has been suggested from the cluster-model analysis<sup>9</sup> as well as the LSDA calculation. The ratio given in Fig. 1 represents the relative photoionization cross section of the Nd  $4f$ , Mn  $3d$ , and O  $2p$  states<sup>22</sup> at the respective photon energy. The intensity around 13 eV is also enhanced in the spectrum at  $h\nu=640$  eV, which is ascribed to the  $e_g$ -derived satellites.<sup>9</sup> However, the hump around 10 eV in the spectrum at  $h\nu=642$  eV is considered as an Auger emission. It is noticed that the Nd  $4f$  components are seen in the off-resonance spectrum taken at  $h\nu=636$  eV, reflecting the relative photoionization cross section of the Nd  $4f$  states. The weakness of the photoemission intensity near 7 eV at  $h\nu=55$  eV is surely due to the reduction of its relative cross section. In this way, the contribution of the rare-earth  $4f$  states should be really taken into account for interpreting the valence-band structures.

Figure 2 shows the temperature-dependent spectra of the  $x=0.47$  and 0.5 samples taken at  $h\nu=55$  eV. There are structures at 0.6, 2.3, 3.0, and 5.6 eV in all the spectra. Comparing the spectra with those in Fig. 1, we conclude that the structures at 3.0 and 5.6 eV mainly originate from the O  $2p$  states, which are not prominent in the spectra at the higher photon-energy excitations. For  $x=0.47$ , there is no remarkable difference in the spectra between 140 and 170 K, both in the FM phase. As for  $x=0.5$ , the gross feature of the spectrum at 140 K is similar to that at 170 K. However, the 2.3 eV structure at 140 K (indicated by an arrow in Fig. 2) is narrower particularly on the lower binding-energy side (2.0–1.6 eV) as revealed in the inset. Furthermore, the narrowing of the 2.3 eV structure itself is more distinct for  $x=0.5$  than for  $x=0.47$ . We consider that the narrowing is caused by the localization of the  $t_{2g}$  states due to the FM-COI transition. It is known that the  $t_{2g}$  levels are split into two levels by the JT distortion, which is thought to become larger in the COI phase as suggested from the temperature dependence of

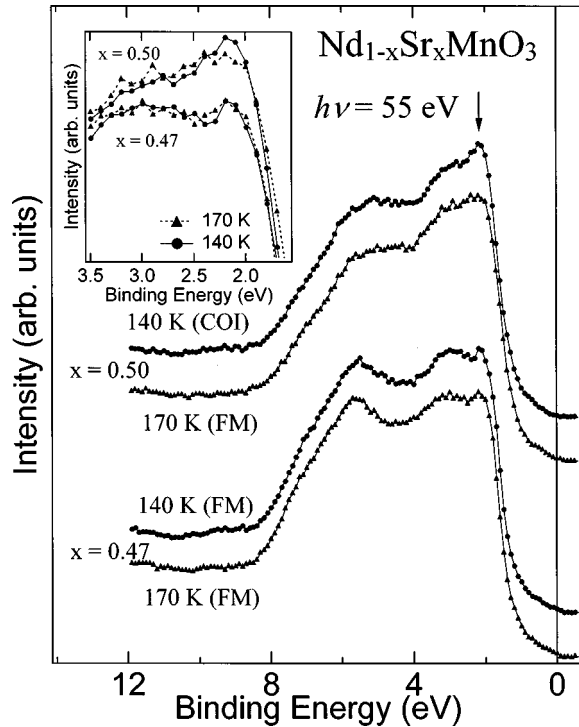


FIG. 2. Valence-band spectra of  $\text{Nd}_{1-x}\text{Sr}_x\text{MnO}_3$  ( $x=0.47, 0.5$ ). The inset: the same spectra on an expanded scale showing the peak-narrowing across the FM-COI transition for  $x=0.5$ .

the lattice parameters.<sup>6</sup> If the energy splitting in the  $t_{2g}$  levels is remarkably larger in the COI phase than in the FM phase, the 2.3 eV structure would broaden at 140 K. In fact, such a broadening is not observed.  $\text{Nd}_{0.5}\text{Sr}_{0.5}\text{MnO}_3$  has the orthorhombic  $O'$  structure even in the FM phase,<sup>6</sup> suggesting that  $t_{2g}$  levels are split in contrast to the case of the FM phase of rhombohedral  $\text{La}_{0.5}\text{Sr}_{0.5}\text{MnO}_3$ . Therefore, it is reasonable to conclude that the  $t_{2g}$  levels are already split in the FM phase and that the energy splitting does not change much between the two phases.

### B. Electronic states near the Fermi level

Temperature dependence of the spectra near  $E_F$  is shown in Fig. 3. The base line for photoemission intensity is shifted between  $x=0.5$  and 0.47. The spectra are normalized by the integrated intensity in the energy region displayed here. In all the spectra, spectral intensities decrease toward  $E_F$ . In the case of  $x=0.47$ , the intensity at  $E_F$  is finite at all temperatures and furthermore a clear Fermi cutoff is observed at 20 K. It should be noted that the spectra for  $x=0.47$  have no essential temperature dependence, which is consistent with that  $\text{Nd}_{0.53}\text{Sr}_{0.47}\text{MnO}_3$  is in the same FM phase irrespective of the temperature. Contrary to this, the spectra of  $x=0.5$  have shown distinct temperature dependence between 140 and 170 K. The spectrum at 140 K is suppressed from  $E_F$  to  $\sim 0.4$  eV and rather enhanced from 0.7 eV to 1.2 eV compared to that at 170 K. At  $E_F$ , the intensity vanishes at 140 K whereas that at 170 K is weak but finite, clearly indicating the opening of the charge-ordering (CO) gap. From the metallic behavior for  $x=0.47$  and the clear FM-COI transition for  $x=0.5$ , we consider that the transition is induced by a subtle competition between the CO instability, which origi-

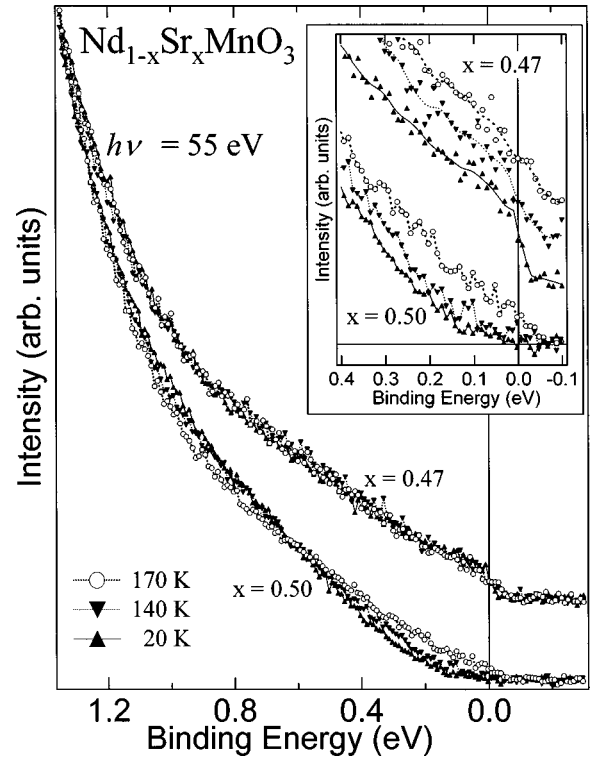


FIG. 3. High-resolution photoemission spectra of  $\text{Nd}_{1-x}\text{Sr}_x\text{MnO}_3$  ( $x=0.47, 0.5$ ) taken at 20, 140, and 170 K near  $E_F$ . The inset shows the spectral changes in the vicinity of  $E_F$ .

nates from the commensurate value of  $x=\frac{1}{2}$ , and the DE interaction. Namely, the DE interaction overcomes the CO instability for incommensurate  $x=0.47$ , making the  $e_g$  bandwidth large enough to become metallic. These spectral behaviors indicate that the electronic states near  $E_F$  rather suddenly change at the FM-COI phase boundary, which is different from the gradual spectral changes toward the transition in the case of the Verwey transition in  $\text{Fe}_3\text{O}_4$ .<sup>23</sup>

Comparing the spectrum for  $x=0.5$  at 20 K with that at 140 K, the intensities around 0.2 eV (1.0 eV) seem to be slightly reduced (enhanced). We have also taken a spectrum at 110 K (not shown), which is identical to that at 20 K. Chainani *et al.* have reported that spectra of  $\text{Pr}_{0.5}\text{Sr}_{0.5}\text{MnO}_3$  show negligible change within the insulating phase.<sup>14</sup> However, their spectra have weak-temperature dependence within the insulating phase, whose tendency is similar to our spectra. From the fact that the resistivity of  $\text{Nd}_{0.5}\text{Sr}_{0.5}\text{MnO}_3$  more rapidly increases with decreasing temperature at 140 K than at 20 and 110 K,<sup>6</sup> we consider that the gap is not completely open at 140 K, which has caused the slight difference between the spectra at 140 K and at lower temperatures. From the spectra in the COI phase, the CO gap (the binding energy of the threshold of finite photoemission intensity) is estimated as about 100 meV at 20 K. This value is smaller than the CO gap estimated by means of a vacuum tunneling spectroscopy study as  $\sim 250$  meV, which is the threshold energy of finite dynamic conductance from the zero-bias voltage corresponding to  $E_F$ .<sup>24</sup> This discrepancy may originate from the methods of the sample preparation, namely, our single crystals are prepared by the floating-zone method while their polycrystalline samples were prepared by the solid-state

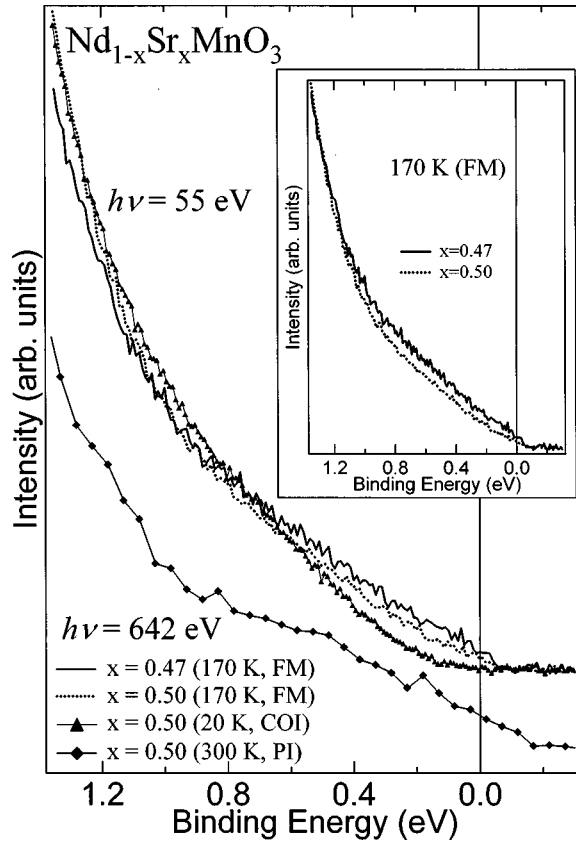


FIG. 4. Filling and photon energy dependence of the spectra near  $E_F$  for  $\text{Nd}_{1-x}\text{Sr}_x\text{MnO}_3$ . The inset shows the comparison between the FM spectra of  $x=0.47$  and  $0.5$  with using different normalization.

method. Indeed, the resistivity and  $T_{COI}$  of their samples are rather different from those of ours.<sup>6,24</sup>

Figure 4 shows a comparison among the spectra near  $E_F$ . The inset of Fig. 4 shows the filling dependence of the spectra, which are normalized to the intensity at the tails of the  $t_{2g}$  spectral weight (from 1.2 to 1.35 eV). The spectra in the main frame are normalized to the integrated intensity from  $E_F$  to 1.35 eV. As for the spectra in the FM phase (at 170 K), the spectral intensity from  $E_F$  to about 1 eV is stronger for  $x=0.47$  than for  $x=0.5$ , which does not depend on the method of normalization. One can also notice that the spectral difference near  $E_F$  between the two  $x$ 's in the FM phase is smaller than that between the FM and COI phases for  $x=0.5$ . The stronger spectral weight from  $E_F$  to  $\sim 1$  eV for  $x=0.47$  itself is reasonable since the mean  $e_g$  electron number is larger for  $x=0.47$  than  $x=0.5$ . If the rigid-band model is appropriate, however, the  $e_g$  band near  $E_F$  for  $x=0.5$  should be shifted toward  $E_F$  compared to that for  $x=0.47$  due to a shift of  $E_F$  within the  $e_g$  band and the spectral weight near  $E_F$  should be higher for  $x=0.5$ . Therefore, the observed filling dependence of the spectra in the FM phase implies that the electron correlation is important for these manganites. As for the Mn  $2p$ - $3d$  resonant photoemission spectrum ( $h\nu=642$  eV), relatively larger spectral weight near  $E_F$  is observed compared to those at  $h\nu=55$  eV. The  $e_g$  contribution is more enhanced in this spectrum than the  $t_{2g}$  and O  $2p$  contributions. Thus, higher-resolution Mn  $2p$ - $3d$  resonant photoemission study is really worth performing in the near future.

Then we discuss the spectral line shapes near  $E_F$  in Fig. 4. At first sight, the overall spectral line shapes are qualitatively similar for  $x=0.47$  and  $0.5$ . The spectrum for  $x=0.5$  at 20 K is regarded as the contribution from the  $e_g$  band that is localized in the COI phase. We, therefore, consider that this spectral weight remains also for  $x=0.47$  as well as for  $x=0.5$  in the FM phases as a reminiscence of the localized  $e_g$  band due to the strong electron correlation. Such a reminiscence is interpreted as a large incoherent spectral weight that originates from the split  $e_g$  band. Several origins are considered for the large incoherent spectral weight, namely, the electron Coulomb interaction combined with the JT distortion,<sup>25</sup> the dynamic JT effect in addition to the DE interaction,<sup>5,26,27</sup> and so on. We consider that the incoherent part in the FM-phase spectra in Fig. 4 near  $x=0.5$  is strongly reflected by these effects. In the present stage, however, it is difficult to quantitatively elucidate how they affect the photoemission spectra near  $E_F$  since reliable band-structure calculations for  $\text{Nd}_{1-x}\text{Sr}_x\text{MnO}_3$  ( $x=0.47,0.5$ ) are lacking. Further theoretical studies as well as higher-resolution photoemission studies are required to clarify this problem.

Finally, we refer to the temperature dependence of the spectra within the FM phase for the perovskite manganese oxide. Our spectra for  $x=0.47$  and the spectra of  $\text{Pr}_{0.5}\text{Sr}_{0.5}\text{MnO}_3$  (Ref. 14) have little temperature dependence while spectra of  $\text{La}_{1-x}\text{A}_x\text{MnO}_3$  ( $A=\text{Sr}$  or  $\text{Ca}$ ) (Refs. 10–13) show remarkable temperature dependence. This experimental discrepancy seems to be related to the difference in the crystal structure between the  $O'$  phase ( $\text{Nd}_{1-x}\text{Sr}_x\text{MnO}_3$ ) and the rhombohedral phase ( $\text{La}_{1-x}\text{Sr}_x\text{MnO}_3$ ). For the rhombohedral manganites, a neutron diffraction study suggests a change of polaron networks with temperature.<sup>27</sup> In the case of  $\text{Nd}_{1-x}\text{Sr}_x\text{MnO}_3$ , however, we consider that the ‘‘intermediate polaron’’ seen in  $\text{La}_{1-x}\text{Sr}_x\text{MnO}_3$  cannot be formed because of the larger  $\text{GdFeO}_3$ -type distortion, and consequently there is no temperature change of the polaron networks. It is understandable that the ‘‘temperature-independent’’ spectra of  $\text{Nd}_{1-x}\text{Sr}_x\text{MnO}_3$  within the FM phase are due to the absence of the change of the polaron networks in contrast to the  $\text{La}_{1-x}\text{A}_x\text{MnO}_3$ .

#### IV. CONCLUSION

We have performed high-resolution temperature-dependent photoemission studies for  $\text{Nd}_{1-x}\text{Sr}_x\text{MnO}_3$  ( $x\sim 0.5$ ). By means of the resonant photoemission, the Nd  $4f$  and Mn  $3d$  contributions to the spectra have been experimentally clarified. By virtue of the high-resolution measurements, we have observed the metallic behavior for  $\text{Nd}_{0.53}\text{Sr}_{0.47}\text{MnO}_3$  in all the measuring temperatures and the FM-COI transition for  $\text{Nd}_{0.5}\text{Sr}_{0.5}\text{MnO}_3$ , where the CO gap has been estimated as about 100 meV. The observed temperature and filling dependence of the spectra near  $E_F$  suggests that the electronic states change rather suddenly at the FM-COI phase boundary and that the electron correlation effect is strong in  $\text{Nd}_{1-x}\text{Sr}_x\text{MnO}_3$  ( $x=0.47,0.5$ ).

#### ACKNOWLEDGMENTS

We are grateful to the staff of PF, especially K. Mamiya, A. Kakizaki, and Y. Azuma for supporting the experiment. We thank K.-S. An, T. Muro, H. Harada, H. Takagi, and M.

Saeki for their technical help. This work was supported by a Grant-in-Aid for COE Research (Grant No. 10CE2004) of the Ministry of Education, Science, Sports, and Culture, Japan, and by the New Energy and Industrial Technology De-

velopment Organization (NEDO). The experiments were performed under the approval of the PF Program Advisory Committee (Proposals Nos. 92S002 and 97G298). A.S. acknowledges support from the Kurata Foundation.

- 
- \*Present address: Japan Synchrotron Radiation Research Institute, Spring-8, Mihara, Mikazuki, Hyogo 679-5198, Japan.
- †Present address: Department of Physics, Sophia University, Chiyoda-ku, Tokyo 102-8554, Japan.
- <sup>1</sup>R. von Helmolt, J. Wecker, B. Holzapfel, L. Shultz, and K. Samwer, *Phys. Rev. Lett.* **71**, 2331 (1993).
- <sup>2</sup>A. Urushibara, Y. Moritomo, T. Arima, A. Asamitsu, G. Kido, and Y. Tokura, *Phys. Rev. B* **51**, 14 103 (1995).
- <sup>3</sup>E. O. Wollan and W. C. Koehler, *Phys. Rev.* **100**, 545 (1955).
- <sup>4</sup>C. Zener, *Phys. Rev.* **82**, 403 (1951); P. W. Anderson and H. Hasegawa, *ibid.* **100**, 675 (1955).
- <sup>5</sup>A. J. Millis, P. B. Littlewood, and B. I. Shraiman, *Phys. Rev. Lett.* **74**, 5144 (1995); A. J. Millis, B. I. Shraiman, and R. Muller, *ibid.* **77**, 175 (1996).
- <sup>6</sup>H. Kuwahara, Y. Tomioka, A. Asamitsu, Y. Moritomo, and Y. Tokura, *Science* **270**, 961 (1995).
- <sup>7</sup>H. Kuwahara, Y. Moritomo, Y. Tomioka, A. Asamitsu, M. Kasai, R. Kumai, and Y. Tokura, *Phys. Rev. B* **56**, 9386 (1997).
- <sup>8</sup>H. Kawano, R. Kajimoto, H. Yoshizawa, Y. Tomioka, H. Kuwahara, and Y. Tokura, *Phys. Rev. Lett.* **78**, 4253 (1997).
- <sup>9</sup>T. Saitoh, A. E. Bocquet, T. Mizokawa, H. Namatame, A. Fujimori, M. Abbate, Y. Takeda, and M. Takano, *Phys. Rev. B* **51**, 13 942 (1995).
- <sup>10</sup>D. D. Sarma, N. Shanthi, S. R. Krishnakumar, T. Saitoh, T. Mizokawa, A. Sekiyama, K. Kobayashi, A. Fujimori, E. Weschke, R. Meier, G. Kaindl, Y. Takeda, and M. Takano, *Phys. Rev. B* **53**, 6873 (1996).
- <sup>11</sup>J.-H. Park, C. T. Chen, S.-W. Cheong, W. Bao, G. Meigs, V. Chakarian, and Y. U. Idzerda, *J. Appl. Phys.* **79**, 4558 (1996).
- <sup>12</sup>J.-H. Park, C. T. Chen, S.-W. Cheong, W. Bao, G. Meigs, V. Chakarian, and Y. U. Idzerda, *Phys. Rev. Lett.* **76**, 4215 (1996).
- <sup>13</sup>T. Saitoh, A. Sekiyama, K. Kobayashi, T. Mizokawa, A. Fujimori, D. D. Sarma, Y. Takeda, and M. Takano, *Phys. Rev. B* **56**, 8836 (1997).
- <sup>14</sup>A. Chainani, H. Kumigashira, T. Takahashi, Y. Tomioka, H. Kuwahara, and Y. Tokura, *Phys. Rev. B* **56**, R15 513 (1997).
- <sup>15</sup>S. Suga and S. Imada, *J. Electron Spectrosc. Relat. Phenom.* **92**, 1 (1998).
- <sup>16</sup>H. Kuwahara (unpublished).
- <sup>17</sup>A. Yagishita, S. Masui, T. Toyoshima, H. Maezawa, and E. Shigemasa, *Rev. Sci. Instrum.* **63**, 1351 (1992).
- <sup>18</sup>S. Masui, E. Shigemasa, and A. Yagishita, *Rev. Sci. Instrum.* **63**, 1330 (1992).
- <sup>19</sup>H. Namatame, A. Fujimori, Y. Tokura, M. Nakamura, K. Yamaguchi, A. Misu, H. Matsubara, S. Suga, H. Eisaki, T. Ito, H. Takagi, and S. Uchida, *Phys. Rev. B* **41**, 7205 (1990).
- <sup>20</sup>A. Fujimori, T. Miyahara, T. Koide, T. Shidara, H. Kato, H. Fukutani, and S. Sato, *Phys. Rev. B* **38**, 7789 (1988).
- <sup>21</sup>N. Hamada, H. Sawada, and K. Terakura, in *Spectroscopy of Mott Insulators and Correlated Metals*, edited by A. Fujimori and Y. Tokura (Springer-Verlag, Berlin, 1995).
- <sup>22</sup>J. J. Yeh and I. Lindau, *At. Data Nucl. Data Tables* **32**, 1 (1985); effects of photoemission resonance are not taken into account for the cross sections displayed in Fig. 1.
- <sup>23</sup>A. Chainani, T. Yokoya, T. Morimoto, T. Takahashi, and S. Todo, *Phys. Rev. B* **51**, 17 976 (1995).
- <sup>24</sup>A. Biswas, A. K. Raychaudhuri, R. Mahendiran, A. Guha, R. Mahesh, and C. N. R. Rao, *J. Phys.: Condens. Matter* **9**, L355 (1997).
- <sup>25</sup>T. Mizokawa and A. Fujimori, *Phys. Rev. B* **51**, 12 880 (1995); **56**, R493 (1997).
- <sup>26</sup>S. G. Kaplan, M. Quijada, H. D. Drew, D. B. Tanner, G. C. Xiong, R. Ramesh, C. Kwon, and T. Venkatesan, *Phys. Rev. Lett.* **77**, 2081 (1996).
- <sup>27</sup>D. Louca, T. Egami, E. L. Brosha, H. Röder, and A. R. Bishop, *Phys. Rev. B* **56**, R8475 (1997).